Since January 2020 Elsevier has created a COVID-19 resource centre with free information in English and Mandarin on the novel coronavirus COVID-19. The COVID-19 resource centre is hosted on Elsevier Connect, the company's public news and information website.

Theriogenology 158 (2020) 309–320

Contents lists available at ScienceDirect

Theriogenology

journal homepage: www.theriojournal.com

Ascorbic acid promotes the reproductive function of porcine immature Sertoli cells through transcriptome reprogramming

Yu-Wei Yang [a], Lu Chen [a], Qiao Mou [a], Hao Liang [b], Zhi-Qiang Du [b, **], Cai-Xia Yang [a, b, *]

[a] College of Animal Science and Technology, Northeast Agricultural University, Harbin, 150030, Heilongjiang, China
[b] College of Animal Science, Yangtze University, Jingzhou, 434025, Hubei, China

ARTICLE INFO

Article history:
Received 9 July 2020
Received in revised form
18 August 2020
Accepted 14 September 2020
Available online 29 September 2020

Keywords:
Pig
Immature Sertoli cell
Ascorbic acid
Transcriptome
Hormone
Metabolite

ABSTRACT

Vitamin C (ascorbic acid, AA) can regulate antioxidation and affect many cellular processes. However, the effect of AA on the reproduction of male animals remains less explored. Here, we showed that by supplementing exogenous AA to porcine immature Sertoli cells (iSCs), AA could promote the proliferation, suppress apoptosis, and decrease the global nucleic acid methylation (5 mC and m^6A) levels of iSCs. After we profiled mRNA and long non-coding RNA (lncRNA) expression by transcriptome sequencing on iSCs (treated by 250 μM AA for 36 h), 1232 mRNAs and 937 lncRNAs were identified to be differentially expressed (DE). Gene enrichment analysis found multiple significantly enriched biological pathways, including oxidoreductase activity, cell proliferation and apoptosis, regulation of hormone level, regulation of catalytic activity, developmental process, ATP metabolism and reproductive process. Specifically, for the reproductive process, 49 up- and 36 down-regulated DE mRNAs (including highly expressed genes, such as *Tfcp2l1, Hmgcs1, Mmp7, Fndc3a,* and *Zfp36l1*) are involved. Moreover, AA supplementation could promote the secretion of anti-müllerian hormone, inhibin B and lactate, and enhance the activity of lactate dehydrogenase as well. Taken together, AA could promote the reproductive function of pig iSCs, potentially through reprogramming the global transcriptome, and elevating hormone secretion and metabolite production.

1. Introduction

Sertoli cell (SC) is an important type of somatic cell of the testis. The swine testicular cell line is established by culturing cells isolated from swine fetal testes (80–90 days) [1,2], which afterwards is characterized as porcine immature Sertoli cells (iSCs) [3]. iSCs cultured *in vitro* are used widely for the study of boar reproduction, especially on how SCs provide physical and nutritional supports to germ cells [4]. Later, SCs are found to be able to secret a variety of molecules, such as growth factors, androgen binding protein (ABP), anti-müllerian hormone (AMH), inhibin B (INHB) and lactate, to provide growth signals and nutrients for spermatogenic cells [5–7]. Furthermore, multiple exogenous factors are discovered to affect the proliferation, apoptosis and function of SCs, including heat stress [8], metal [7,9], chemicals [5] and nutrients [10], and disturb the subsequent development of germ cells [7].

Vitamin C (ascorbic acid, AA) is an essential micronutrient, and of vital roles to many physiological and biochemical processes, including the reproduction of male animals. AA treatment could reverse the testicular damages in diabetic rats [11]. AA supplement improves the differentiation of testicular cells, ultimately increasing the cell number and stimulating sperm production [12]. Moreover, AA could effectively improve the integrity of sperm DNA of human patients [13], and also the quality of frozen bull semen [14]. Accumulating evidences indicate that AA treatment could benefit the male reproductive system (organs and cells) at different layers of action. First, AA could increase the concentration of glutathione (GSH) [15], neutralize the reactive oxygen species (ROS) [16], and regulate the activity of multiple enzymes involved in the oxidation-reduction pathway [17,18]. Second, AA can also reprogram the epigenomic status [19], such as histone acetylation [20], DNA [18] and RNA methylation [21]. Third, AA could orchestrate the gene expression network [22], including microRNAs (miRNAs) [23], piwi-interacting RNAs (piRNAs) [24] and long non-coding RNAs

* Corresponding author. College of Animal Science and Technology, Northeast Agricultural University, Harbin, 150030, Heilongjiang, China.
** Corresponding author.
E-mail addresses: zhqdu@yangtzeu.edu.cn (Z.-Q. Du), caixiayang@neau.edu.cn (C.-X. Yang).

https://doi.org/10.1016/j.theriogenology.2020.09.022
0093-691X/

(lncRNAs) [25]. However, the exact molecular mechanism underlying the effects of AA on male reproductive cells remains largely unknown.

In the present study, using *in vitro* cultured porcine iSCs, we first assessed the effect of exogenous supplementation of AA on the proliferation, apoptosis and nucleic acid methylation. Then, transcriptome sequencing (mRNAs and lncRNAs) was performed to profile the transcriptional changes induced by AA treatment, to reveal important genes and molecular pathways contributing to the observed phenotypic changes of iSCs. Lastly, to validate the functional outcomes of iSCs induced by AA supplementation, we assayed the secretion of key hormones (AMH and INHB), the activity of an important enzyme (LDH) and also the level of its metabolite (lactate).

2. Materials and methods

2.1. Ethics statement

All experiments were approved by the Animal Care Commission and Ethics Committee of Northeast Agricultural University, China.

2.2. Cell culture and AA treatment

The swine testicular cell line was purchased from the American Type Culture Collection (ATCC® CRL-1746™), which has been isolated from fetal testes (80–90 days in gestation), and characterized as the porcine immature Sertoli cells (iSCs) [3]. iSCs were cultured in a 5% CO_2 incubator at 37 °C, in the Minimum Essential Medium (MEM) with Eagle's balanced salt solution (HyClone, USA), supplemented with 10% fetal bovine serum (Clark, Australia) and 1% penicillin-streptomycin (Gibco, USA). Cells were seeded at a density of 1×10^5 cells/mL, and cultured for 6 h, before treating with AA. In the present study, derivative of L-ascorbic acid, L-ascorbic acid 2-phosphate sesquimagnesium salt hydrate (AA2P; A8960; Sigma, St. Louis, MO, USA) was used, to avoid degradation due to the heat and light exposure [21]. AA2P was added into the medium at the final concentrations as desired (0, 100 μM, 250 μM and 500 μM). Then, we assessed the data of cell proliferation and chose the optimal concentration of AA2P for further investigation.

2.3. Cell proliferation

Cells were seeded in a 96-well plate at a density of 1×10^4 cells per well, and allowed to grow for 6 h. After AA2P (0, 100 μM, 250 μM and 500 μM) treatment of cells for 0, 24 h, 36 h and 48 h, 10 μL of thiazolyl blue tetrazolium bromide (5 mg/mL in PBS) (Sigma, USA) were added into the culture media, and continued the cell culture for 4 h. The plate with cells was centrifuged at 1800 rpm for 10min, and the supernatant was removed, followed by adding 150 μL of dimethyl sulfoxide and incubating for 15min. Cell viability was determined at 570 nm using a 96-cell plate reader (Bio-Rad 680, USA).

2.4. Cell cycle

Approximately 2×10^5–1×10^6 cells were collected from the control or 250 μM AA2P-treated (36 h) groups, respectively, and then treated using the cell cycle staining kit (CCS01, MultiSciences Biotech Co., Ltd, Hangzhou, China) according to the manufacturer's instruction. Briefly, cells were centrifuged and re-suspended in 1 mL DNA staining solution (propidium iodide) and 10 μL permeabilization solution. After vortexing for 5–10sec, cells were incubated in dark for 30min. Finally, cells were subjected to flow cytometry (BD AiraII, USA) to determine the stages of cell cycle.

2.5. ROS, mitochondrial distribution/membrane potential and apoptosis

Cells were seeded in 24-well plates at a density of 1×10^5 cells per well, cultured and treated using AA2P as described above. After the culture medium was removed, cells were incubated with 10 μM 2′, 7′-dichlorodihydrofluorescein diacetate or 5 μg/mL Rhodamine 123 (RH123) in PBS for 30 min at 37 °C in dark, to assay the ROS level and mitochondrial membrane potential. Following three washes with serum-free culture medium, fluorescence images of cells were taken under the inverted fluorescence microscope (Olympus, Tokyo, Japan). Five images were taken under the same setting parameters from five different areas of each sample, and quantification of fluorescence was done using the Image J (version 1.48 V; NIH, Bethesda, MD, USA) software. The relative fluorescence intensity was calculated by treating the control group as the standard reference.

To evaluate the mitochondrial distribution, cells were grown till 30–40% confluence. Then, cells were stained with 100 nM Mito-Tracker Green dye (M7514; Invitrogen, Paisley, UK) at 37 °C for 30min in dark. The nuclei of cells were stained with Hoechst33342. Fluorescent images at emission of 488 nm were captured using a laser scanning confocal microscope (Leica, Germany). The Image J software was used to measure the fluorescence intensity of Mito-Tracker Green staining as described above.

Cell apoptosis was analyzed by the Annexin V-FITC Apoptosis Detection Kit (Vazyme, Nanjing, China) according to the manufacturer's instruction. Briefly, 10^6 cells approximately were harvested and washed twice using PBS. Then, cells were incubated for 10 min at 37 °C with Annexin V-FITC (1:100 in binding buffer) and propidium iodide solution. Cells were subjected to flow cytometry (BD AiraII, USA), and the proportion of cells with positive apoptotic signal was calculated.

2.6. Nucleic acid methylation

Cells were cultured on coverslips and treated with AA2P for 36 h, before subjected to immunostaining according to a previously described method [26], with some modifications. Cells were fixed in 4% paraformaldehyde for 15min, permeabilized with 0.2% TritonX-100 for 3 h, and blocked with 2% bovine serum albumin (BSA) for 1 h. Overnight incubation was performed with the rabbit anti-N6-methyladenosine (m^6A) monoclonal antibody (1:100; ab190886; Abcam) at 4 °C, followed by three PBS washes containing 0.05% Tween-20 (5min each). Secondary antibody (FITC conjugated goat anti-rabbit IgG (H + L); HS111; TransGen. Biotech) was diluted (1:300) to incubate samples for 1 h at room temperature. After washing, cells were stained with Hoechst33342 (10 μg/mL) for 10min. Finally, coverslips with cells were placed upside down onto glass slides in the ProLong Diamond Antifade Mountant reagent (Life Technologies, USA). Negative controls were those that incubated without primary or secondary antibodies. Images were taken using a laser-scanning confocal microscope (Leica, Germany) and the Image J software was used to quantify the fluorescence intensity of cells as decribed above.

To detect the level of N5-methylcytidine (5 mC), we slightly modified the above protocol. Samples were treated with 4 N HCl for 50 min at 37 °C followed by 4 washes in 0.05% Tween-20. Then, cells were blocked for 1 h in PBS containing 2% BSA, and incubated with anti-5mC polyclonal antibody (1:150; A2341; ABclonal) overnight at 4 °C.

2.7. RNA-seq and data analysis

Total RNA samples were collected from three controls (C1, C2

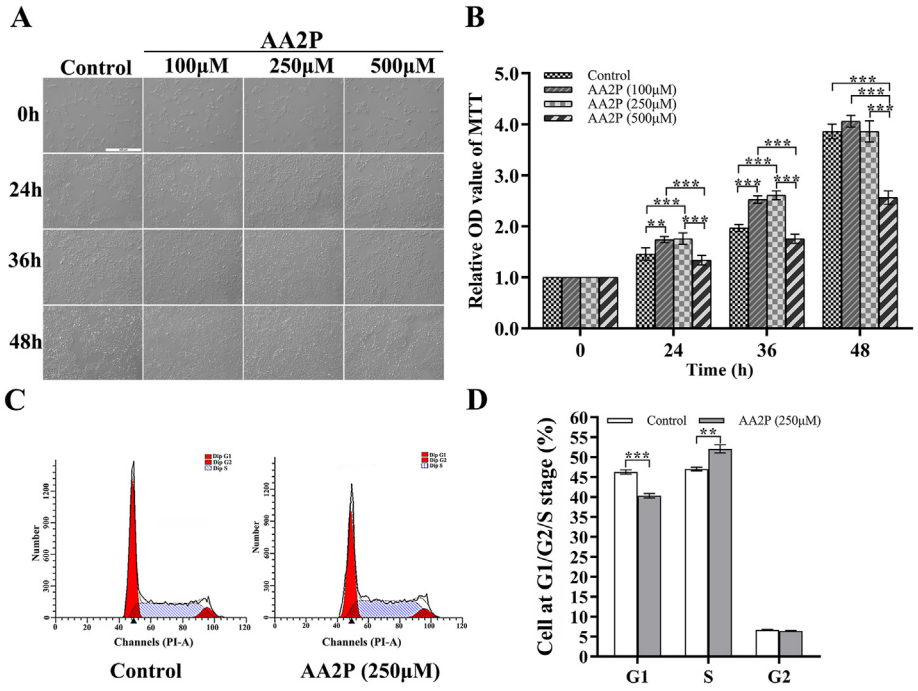

Fig. 1. Effects of AA2P on the proliferation and cell cycle of porcine iSCs. (A) Representative images of cells after treating with different concentrations of AA2P, and then cultured for different lengths of time. Scale bar: 500 μm. (B) Relative OD values to show the proliferation of cells after treatment of AA2P at different concentrations for different time periods. (C) Representative images obtained using flow cytometry to show the phase distribution of cell cycles (G1, S and G2), of cells treated with or without AA2P (250 μM) and cultured for 36 h. (D) Graphs to show the proportion of cells distributed in different phases of cell cycle (G1, S and G2). *, significant difference at $P < 0.05$ level; **, at $P < 0.01$; and ***, at $P < 0.001$. Abbreviations:AA2P, L-ascorbic acid 2-phosphate sesquimagnesium salt hydrate; iSCs, immature Sertoli cells; OD, optical density.

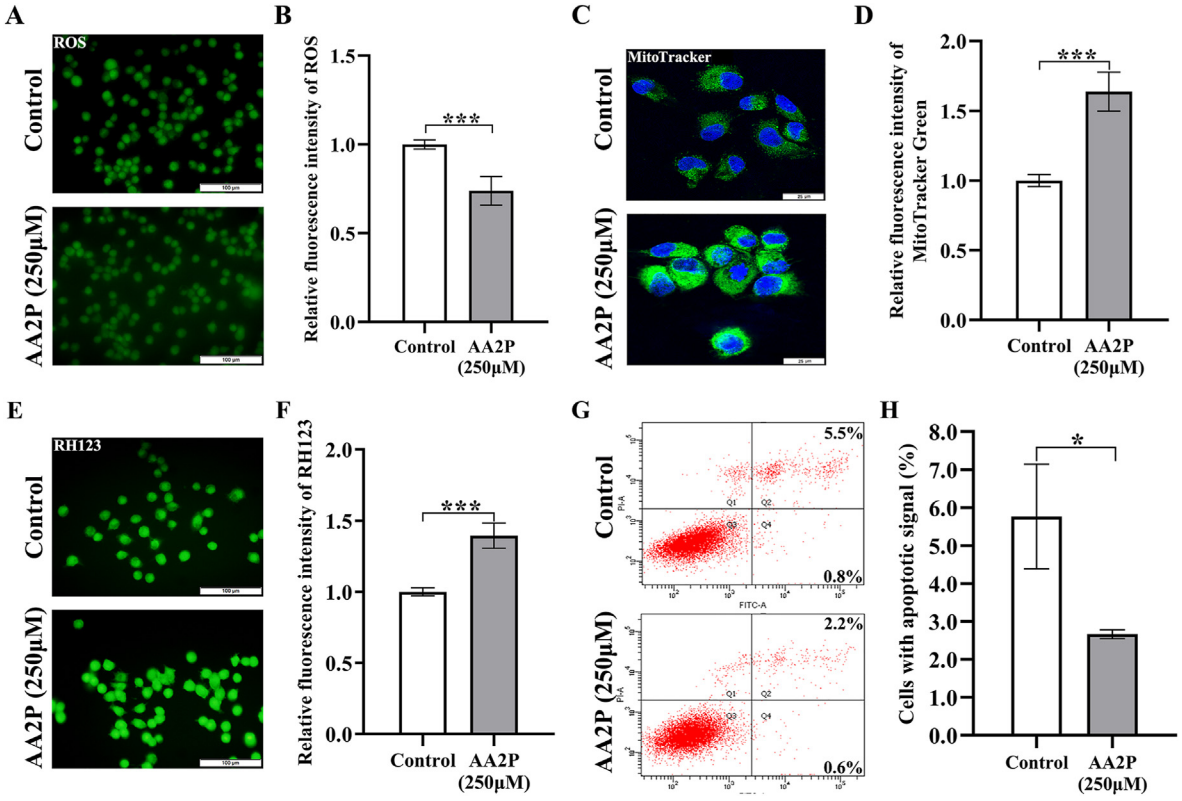

Fig. 2. ROS level, mitochondrial features and apoptosis of iSCs treated by AA2P. (A, C, E) Representative images of ROS, MitoTracker and RH123 staining. Scale bar: 100 μm for ROS and RH123 staining, 25 μm for MitoTracker staining. (B, D, F) Relative fluorescence intensities of ROS, MitoTracker and RH123 staining. (G) Representative images obtained using flow cytometry to show the distribution of apoptotic cells treated with or without AA2P (250 μM) for 36 h. (H) Graphs to show the apoptotic proportion of cells. Abbreviations:RH123, Rhodamine 123; ROS, Reactive oxygen species.

and C3) and three AA2P-treated (V1, V2 and V3) porcine iSCs using the Trizol reagent (Sigma). The libraries were constructed and sequenced on the Illumina HiSeq 2000 platform (Illumina, San Diego, CA, USA) in a single lane. After removal of low-quality and adaptor containing reads, the remaining reads were further aligned against the pig genome (Sscrofa11.1) by the HISAT2 software (v2.0.5) [27]. Detailed information on the generated short reads could be found in Table S1. Following alignment, transcripts were assembled by StringTie (v1.3.2d), expression level of each gene was quantified with FPKM (fragments per kilobase million) [28]. Differentially expressed genes (DEGs) were identified by DEseq (v1.16.0) (http://www.bioconductor.org/packages/release/bioc/html/DESeq.html) based on the reads count file obtained by HTSeq (v0.6.0), and a gene was considered significant if the Benjamini and Hochberg–adjusted P value (Padj.) was <0.05 and the $|\log_2$fold change| was ≥1. DEGs were submitted for enrichment analysis by the Gene Ontology (GO) and KEGG (Kyoto Encyclopedia of Genes and Genomes) tools [29]. RNA-seq raw data have been deposited in NCBI GEO with accession number as GSE153157.

2.8. Hormones, enzymatic activity and lactate

The media for porcine iSC culture with or without AA2P treatment were collected, centrifuged and then used to analyze the levels of anti-mullerian hormone (Langdun, Shanghai, China) and inhibin B (Langdun), according to the manufacturer's instructions. Briefly, 50 μL standard sample was added into each test well with 50 μL supernatant medium. Then, after 50 μL biotin antigen working fluids were added into all wells, the plate was covered with membrane and incubated for 1 h at 37 °C. Following 5 washes (30sec each) using the washing solution, 50 μL avidin-HRP was added into each well and incubated for 30 min at 37 °C. After another wash, 50 μL chromogenic reagents A and B were added and incubated for 10 min at 37 °C in dark. Finally, 50 μL stop solution was added into each well. After a swift shake, absorbance values were obtained using a microplate reader (Bio-Rad 680, USA) at 450 nm.

To detect the activity of lactate dehydrogenase (LDH), cells were treated first by the lysis buffer, and centrifuged for 10 min at 12000 rpm/min to collect the supernatant, which was then used to measure the LDH activity using a commercial kit (Jiancheng, Nanjing, China), according to the manufacturer's instructions. Briefly, after adding 25 μL matrix buffer into the well with 55 μL ddH_2O and 20 μL sample, the plate was shaken and incubated for 15 min at 37 °C in dark. Then, the NaOH solution (250 μL 0.4 M) was added into the well and absorbance values were detected using a microplate reader (Bio-Rad 680, USA) at 450 nm.

For the level of lactate, the culture medium was collected and used for the measurement using a commercial kit (Jiancheng, Nanjing, China), according to the manufacturer's instructions. Briefly, 1 mL of enzyme working solution and 200 μL chromogenic reagents were added into the tube, and mixed well with 20 μL medium sample, which were then incubated for 10 min at 37 °C in dark. Afterwards, 2 mL stop solution was added into the tube to stop the reaction and then shaken briefly. Finally, 200 μL mixture was transferred into a 96-well plate and the absorbance values

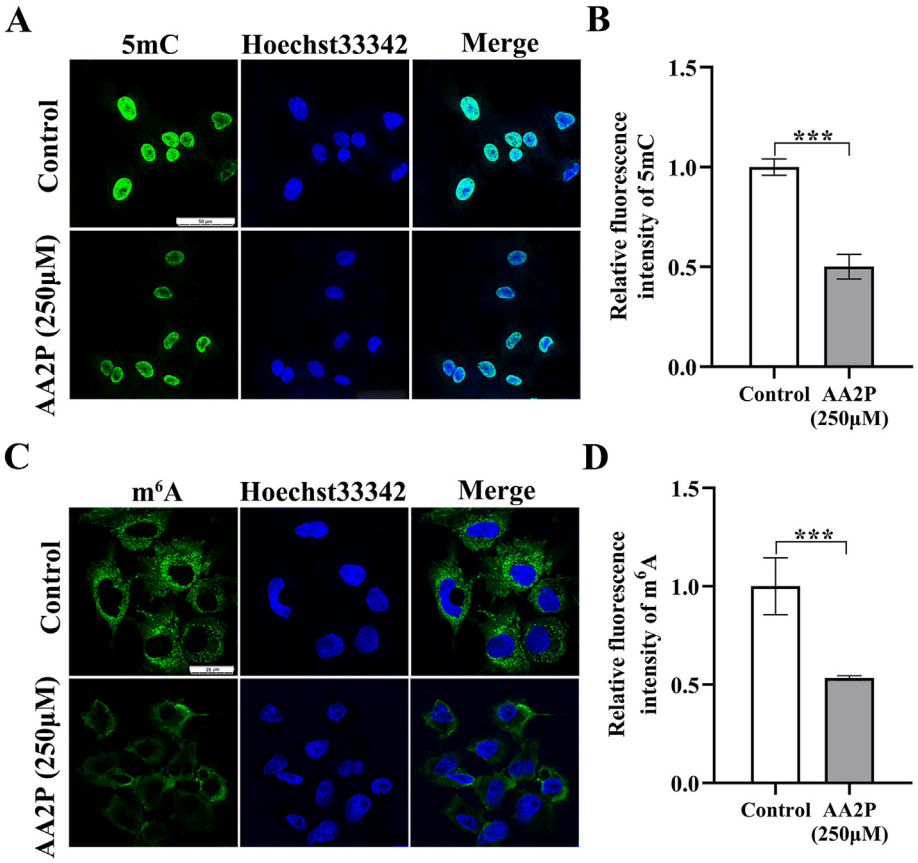

Fig. 3. AA2P and global methylation level of nucleic acids. (A, C) Immunofluorescence images of 5 mC and m^6A staining in porcine iSCs treated with or without AA2P (250 μM) for 36 h. Green, 5 mC and m^6A; Blue, Hoechst33342. Scale bar: 50 μm for 5 mC staining and 25 μm for m^6A staining. (B, D) Relative fluorescence intensity analysis of 5 mC and m^6A levels. Abbreviations:5 mC, N5-methylcytidine; m^6A, N6-methyladenosine. (For interpretation of the references to colour in this figure legend, the reader is referred to the Web version of this article.)

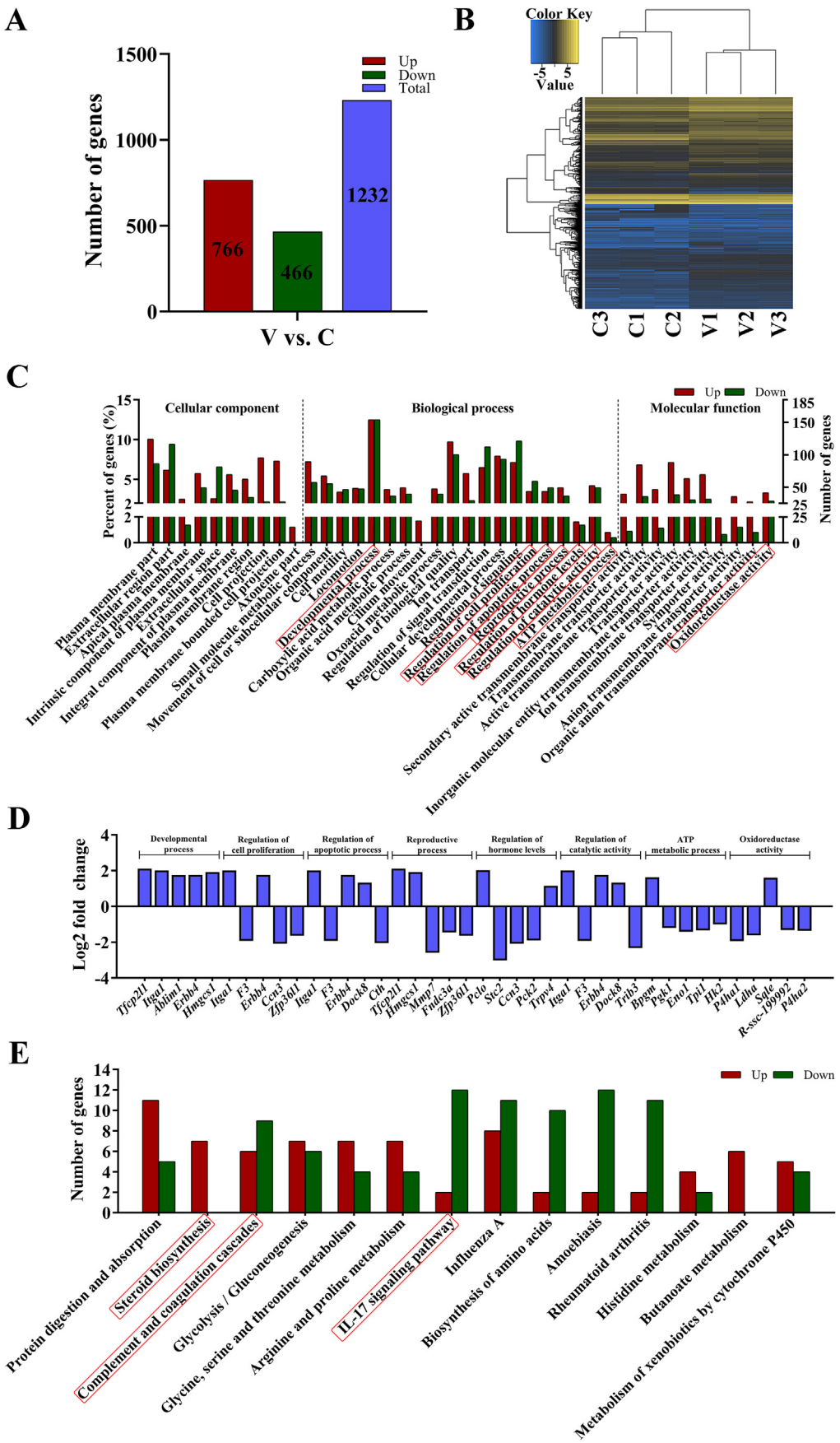
A
Number of genes
1500
1000
500
0
Up
Down
Total
766
466
1232
V vs. C
B
Color Key
-5 5
Value
C3
C1
C2
V1
V2
V3
C
Cellular component
Biological process
Molecular function
Up
Down
Percent of genes (%)
Number of genes
Plasma membrane part
Extracellular region part
Apical plasma membrane
Intrinsic component of plasma membrane
Extracellular space
Integral component of plasma membrane
Plasma membrane region
Plasma membrane bounded cell projection
Cell projection
Axoneme part
Movement of cell or subcellular component
Cell motility
Locomotion
Developmental process
Carboxylic acid metabolic process
Organic acid metabolic process
Oxoacid metabolic process
Regulation of biological quality
Cilium movement
Cellular developmental process
Ion transport
Regulation of signal transduction
Regulation of cell proliferation
Regulation of signaling
Regulation of apoptotic process
Reproductive process
Regulation of hormone levels
Regulation of catalytic activity
ATP metabolic process
Transmembrane transporter activity
Secondary active transmembrane transporter activity
Active transmembrane transporter activity
Inorganic molecular entity transmembrane transporter activity
Ion transmembrane transporter activity
Anion transmembrane transporter activity
Organic anion transmembrane transporter activity
Oxidoreductase activity
D
Log2 fold change
Developmental process
Regulation of cell proliferation
Regulation of apoptotic process
Reproductive process
Regulation of hormone levels
Regulation of catalytic activity
ATP metabolic process
Oxidoreductase activity
Tfcp2l1 Itgal Ablim1 Erbb4 Hmgcs1 Itgal F3 Erbb4 Ccn3 Zfp36l1 Itgal F3 Erbb4 Dock8 Cth Tfcp2l1 Hmgcs1 Mmp7 Fndc3a Zfp36l1 Pclo Stc2 Ccn3 Pck2 Trpv4 Itgal F3 Erbb4 Dock8 Trib3 Bpgm Pgk1 Eno1 Tpi1 Hk2 P4ha1 Ldha Sqle R-ssc-199992 P4ha2
E
Number of genes
Up
Down
Protein digestion and absorption
Steroid biosynthesis
Complement and coagulation cascades
Glycolysis / Gluconeogenesis
Glycine, serine and threonine metabolism
Arginine and proline metabolism
IL-17 signaling pathway
Influenza A
Biosynthesis of amino acids
Amoebiasis
Rheumatoid arthritis
Histidine metabolism
Butanoate metabolism
Metabolism of xenobiotics by cytochrome P450

were measured using a microplate reader (Bio-Rad 680, USA) at 530 nm.

Blank wells were set for each experiment. Each sample was set in triplicates to minimize the technical error.

2.9. Statistical analysis

Statistical analyses were performed by the one-way ANOVA followed by the Duncan's test, using SPSS22.0 software (SPSS Inc, Chicago, IL). At least three biological replicates were performed for each experiment, and the results were expressed as mean ± SEM. Significant differences at $P < 0.05$, 0.01 and 0.001 were indicated as *, ** and ***, respectively.

3. Results

3.1. AA2P promotes cell proliferation

After porcine iSCs were treated for 24 h, 36 h and 48 h, respectively, by adding AA2P (0, 100 μM, 250 μM and 500 μM) into the culture media, we observed the quick proliferative rates of cells in 100 μM and 250 μM AA2P-treated groups (Fig. 1A). The proliferation assay showed that at 100 μM (for 24 h, 1.74 vs. 1.45 of the control, $P < 0.01$, and for 36 h, 2.52 vs. 1.97 of the control; $P < 0.001$), and 250 μM (for 24 h, 1.76 vs. 1.45 of the control, $P < 0.001$; and for 36 h, 2.61 vs. 1.97 of the control, $P < 0.001$), AA2P treatment could significantly promote the proliferation of iSCs (Fig. 1B), respectively. However, 500 μM AA2P treatment could have negative effects and inhibit the cell growth significantly (2.56 vs. 3.86 of the control at 48 h; $P < 0.001$) (Fig. 1B). Thus, exogenous AA2P treatment at a proper concentration could promote the proliferation of porcine iSCs. For subsequent experiments, 250 μM AA2P and 36 h were chosen as the optimized concentration and length of treatment time.

Furthermore, we analyzed the distribution of cell cycle following 250 μM AA2P treatment on iSCs for 36 h (Fig. 1C). Our results showed that AA2P treatment could reduce significantly the proportion of cells in the G1 phase (40.34% vs. 46.30% of the control group; $P < 0.001$). On the contrary, the S phase cells increased significantly (52.09% vs. 47.01% of the control group; $P < 0.01$) (Fig. 1D). Therefore, AA2P treatment could change the cell cycle distribution, by promoting the entry of more cells into the S phase and out from the G1 phase, thereby to accelerate cell proliferation.

3.2. AA2P inhibits apoptosis

To determine the effect of AA2P treatment on iSC apoptosis, we first checked the ROS level (Fig. 2A). The results showed that the ROS level could be significantly decreased by 250 μM AA2P treatment for 36 h (0.74 vs. 1.00 of the control group; $P < 0.001$) (Fig. 2B). Further assessment of mitochondrial features demonstrated that AA2P supplementation could also elevate the number of mitochondria (1.64 vs. 1.00; $P < 0.001$) (Fig. 2C and D) and the mitochondrial membrane potential (1.39 vs. 1.00; $P < 0.001$) (Fig. 2E and F) both to a highly significant level, as compared to the control group. Next, we detected the apoptotic signal using cell cytometry, and found that the proportion of cells with apoptosis in AA2P treatment group was significantly lower than that of the control group (2.67% vs. 5.77%; $P < 0.05$) (Fig. 2G and H). Taken together, AA2P could inhibit the apoptosis of iSCs via reducing the ROS level and enhancing the mitochondrial function.

3.3. AA2P reduces the global level of nucleic acid methylation

Previously, AA2P has been shown to regulate the levels of both DNA 5 mC methylation [18] and RNA m^6A methylation [21]. We determined also the global level of nucleic acid methylation (Fig. 3A and C), and the results showed that in porcine iSCs, AA2P treatment (250 μM, 36 h) could significantly reduce both the DNA 5 mC level (0.50 vs. 1.00; $P < 0.001$) (Fig. 3B), and the RNA m^6A level (0.53 vs. 1.00; $P < 0.001$) (Fig. 3D). Thus, AA2P could reduce both m^6A and 5 mC levels of nucleic acids in a global fashion, suggesting epigenetic modifications were involved in the cellular reprogramming of iSCs treated by AA2P.

3.4. AA2P induces transcriptome changes

In order to further explore the molecular mechanism underlying AA2P-mediated effects on porcine iSCs, transcriptome sequencing was performed, and a total of 17,670 mRNAs were detected in the porcine iSC cell line. We identified that 1232 mRNAs were significantly differentially expressed (DE) ($|\log_2$fold change$| \geq 1$ and Padj.<0.05; Table S2), in which 766 and 466 were up- and down-regulated in AA2P-treated group, respectively (Fig. 4A). Heatmap analysis showed that two separate groups of three AA2P treated and three control samples were formed, respectively, suggesting good reliability of the data obtained (Fig. 4B). Gene enrichment analysis of DE mRNAs found multiple biological processes, including cell proliferation, reproductive process, developmental process, biological regulation, catalytic activity, antioxidant activity, and transcription regulator activity (Fig. 4C). For each of the selected important biological processes, the top five DE mRNAs (Normalized expression$\geq$100) were listed (starting from the mRNA with the smallest P value), including genes of vital roles, such as *Tfcp2l1, Erbb4, Ccn3, Mmp7,* and *Sqle* (Fig. 4D). GO terms (reproductive process and regulation of hormone levels) were enriched from 85 DE mRNAs (49 up- and 36 down-regulated) and 37 DE mRNAs (20 up- and 17 down-regulated), respectively (Table S3). KEGG analysis of DE mRNAs also found multiple signal pathways of potential importance, such as steroid biosynthesis, IL-17 signal pathway, and complement and coagulation cascade (Fig. 4E; Fig. S1).

Furthermore, we analyzed the transcriptional levels of vital genes known to be related to AA incorporation and phenotypic alteration induced by AA2P treatment on porcine iSCs (Table S4). Both *Svct1* and *Svct2* (vitamin C transporters) were found to be expressed in porcine iSCs, with *Svct1* at lower and *Svct2* at higher levels, respectively. After AA treatment (250 μM, 36 h), *Svct1* significantly increased by 3.71 fold (Padj.<0.05), whereas *Svct2* plummeted around 40.7%. For DNA methylation related enzymes, only *Dnmt3l* showed significant decrease by 66% ($|\log_2$fold change$| \geq 1$ and Padj.<0.05). *Dnmt3b* increased 1.56 folds (Padj.<0.05), but *Tet 1* and *Tet 3* decreased to 0.85 and 0.71 folds (Padj.<0.05), respectively, after AA2P treatment (all showing transcriptional levels not larger than 2 folds). Similarly, for enzymes related to RNA m^6A methylation, *Fto* increased 1.18 fold (Padj.<0.01; Table S4). Interestingly, angiotensin-converting enzyme 2 (*Ace2*), the receptor reported of the pandemic new corona virus (2019-

Fig. 4. AA2P changes mRNA expression and associated molecular pathways. (A) Number of differentially expressed (DE) mRNAs in AA2P-treated porcine iSCs as compared to control cells as detected by RNA-seq ($|\log_2$fold change$| \geq 1$ and Padj.<0.05). (B) Heatmap of mRNA expression, showing that AA2P-treated and control samples were clearly clustered into two separate groups. (C) GO terms significantly enriched ($P < 0.05$). (D) Top five DE mRNAs (Normalized expression$\geq$100, beginning from the smallest P value) in each selected GO terms, as listed in (C) with red frames. (E) KEGG signaling pathways significantly enriched ($P < 0.05$). (For interpretation of the references to colour in this figure legend, the reader is referred to the Web version of this article.)

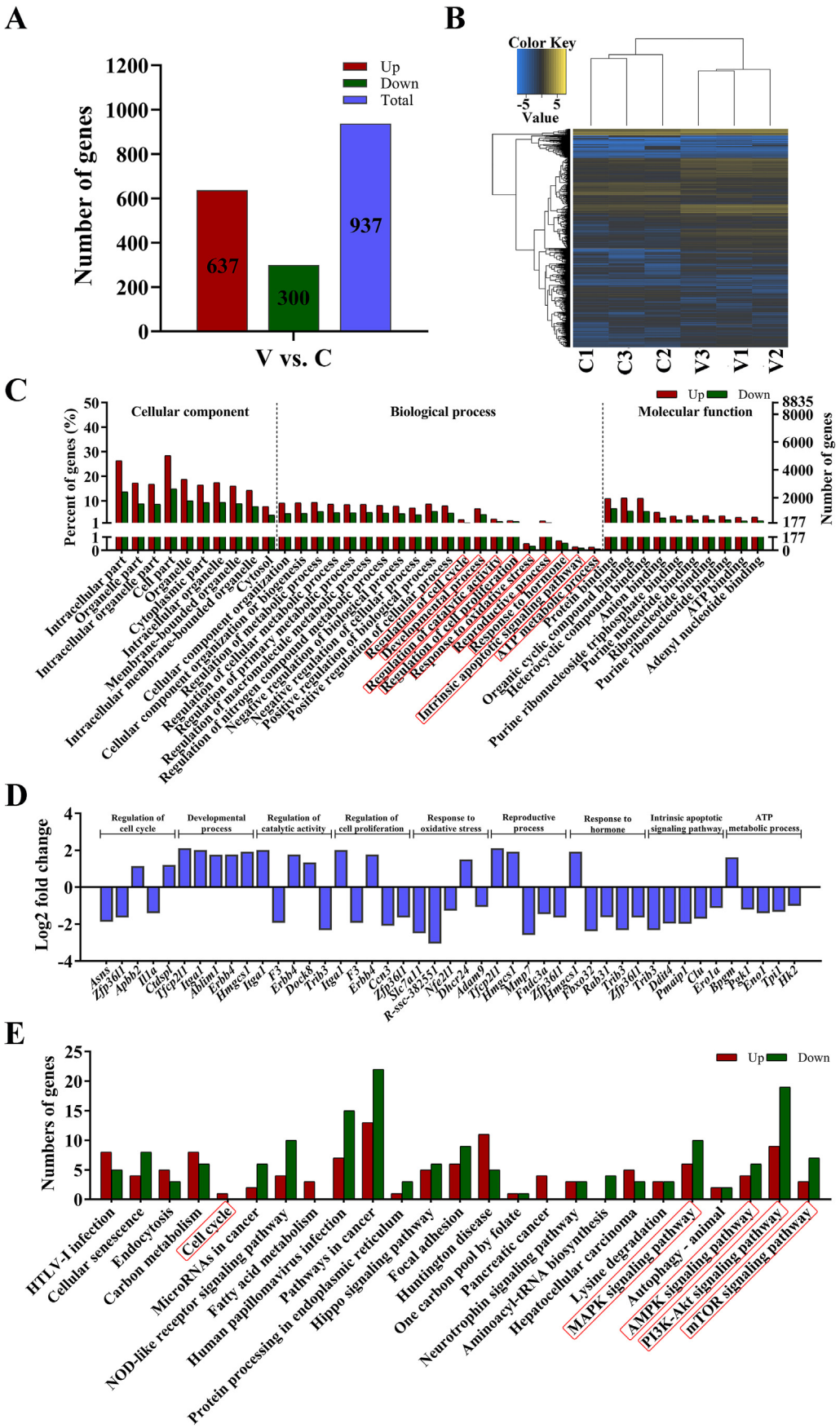
A
Number of genes
Up
Down
Total
637
300
937
V vs. C
B
Color Key
-5 5
Value
C1 C3 C2 V3 V1 V2
C
Up Down
Percent of genes (%)
Number of genes
Cellular component
Biological process
Molecular function
Intracellular part
Organelle part
Intracellular organelle part
Cell part
Organelle
Cytoplasmic part
Intracellular organelle
Membrane-bounded organelle
Intracellular membrane-bounded organelle
Cytosol
Cellular component organization or biogenesis
Intracellular organization
Membrane-bounded organelle
Cellular component organization
Regulation of cellular metabolic process
Regulation of primary metabolic process
Regulation of macromolecule metabolic process
Regulation of nitrogen compound metabolic process
Negative regulation of biological process
Positive regulation of biological process
Regulation of cellular process
Regulation of biological process
Regulation of cell cycle
Developmental process
Regulation of catalytic activity
Regulation of cell proliferation
Response to oxidative stress
Reproductive process
Response to hormone
ATP metabolic process
Protein binding
Organic cyclic compound binding
Heterocyclic compound binding
Anion binding
Purine ribonucleoside triphosphate binding
Purine nucleotide binding
Ribonucleotide binding
Purine ribonucleotide binding
ATP binding
Adenyl nucleotide binding
D
Log2 fold change
Regulation of cell cycle
Developmental process
Regulation of catalytic activity
Regulation of cell proliferation
Response to oxidative stress
Reproductive process
Response to hormone
Intrinsic apoptotic signaling pathway
ATP metabolic process
Asns Zfp36l1 Apbb2 Il1a Ctdspl Tfcp2l1 Itga1 Ablim1 Erbb4 Hmgcs1 Itga1 F3 Erbb4 Dock8 Trib3 Itga1 F3 Erbb4 Ccn3 Zfp36l1 Slc7a11 R-ssc-382551 Nfe2l1 Dhcr24 Adam9 Tfcp2l1 Hmgcs1 Mmp7 Frdc3a Zfp36l1 Hmgcs1 Foxo32 Ran31 Trib3 Zfp36l1 Trib3 Ddit4 Pmaip1 Clu Ero1a Bpsgm Pgk1 Eno1 Tpi1 Hk2
E
Numbers of genes
Up Down
HTLV-I infection
Cellular senescence
Endocytosis
Carbon metabolism
Cell cycle
MicroRNAs in cancer
NOD-like receptor signaling pathway
Fatty acid metabolism
Human papillomavirus infection
Pathways in cancer
Protein processing in endoplasmic reticulum
Hippo signaling pathway
Focal adhesion
Huntington disease
One carbon pool by folate
Pancreatic cancer
Neurotrophin signaling pathway
Aminoacyl-tRNA biosynthesis
Hepatocellular carcinoma
Lysine degradation
MAPK signaling pathway
Autophagy - animal
AMPK signaling pathway
PI3K-Akt signaling pathway
mTOR signaling pathway

nCov), was found to be expressed also in porcine iSCs. AA2P treatment (250 μM, 36 h) significantly increased the level of *Ace2* to a 5.28 fold (Table S4; Padj.<0.05). Therefore, RNA-seq could help to understand the transcriptional changes induced by AA2P supplementation on porcine iSCs.

One report showed that AA treatment of donor cell could restore the expression of some lncRNAs in cloned embryos [25], suggesting the link between AA and lncRNA expression. Similar to mRNAs, certain lncRNAs contain also the poly-A tails that could be amplified and detected by transcriptome sequencing. In the present study, a total of 10,082 lncRNAs were detected in porcine iSCs (3347 known and 6735 novel lncRNAs). We found that 937 lncRNAs (221 known and 716 novel) were significantly differentially expressed ($|\log_2$fold change$|\geq 1$; Padj.<0.05; Table S5), within which 637 (165 known and 472 novel) and 300 (56 known and 244 novel) were up- and down-regulated in AA2P-treated group (Fig. 5A), respectively. After heatmap analysis of lncRNA expression, the treatment and control groups were separately clustered together (Fig. 5B), consistent with the results obtained by mRNA clustering analysis. Gene enrichment analysis of genes targeted by DE lncRNAs also found multiple biological processes, including regulation of cell cycle, developmental process, regulation of catalytic activity, reproductive process, response to hormone, intrinsic apoptotic signaling pathway, and ATP metabolic process (Fig. 5C). The top five mRNA targets for each biological process (Normalized expression≥100; starting first from the gene with the smallest P value) were listed (Fig. 5D), including *Tfcp2l1, Erbb4* and *Ccn3,* as mentioned above after DE mRNA analysis. KEGG analysis also found various signaling pathways, including MAPK, AMPK, PI3K-AKT, mTOR, Wnt, TNF, and Insulin signaling pathways (Fig. 5E; Fig. S2). In addition, further mRNA-lncRNA network analysis also showed the relationship between differentially expressed lncRNAs and their target mRNAs, potentially underlying the molecular expressional changes as induced by AA2P treatment on porcine iSCs, which awaits further investigation (Fig. 6).

3.5. AA2P promotes the secretion of reproductive hormones and metabolite

It is well accepted that iSCs could secret multiple hormones and metabolites, such as AMH, INHB and lactate, to nourish and support spermatogenesis [4,5]. In addition, after transcriptome sequencing on iSCs treated by AA2P, we found also biological and signaling pathways related to hormone response, reproductive processes. Hence, we performed validation assays on the levels of those secreted substances (AMH, INHB and lactate), and also the activity of LDH. Interestingly, AA2P treatment (250 μM, 36 h) significantly increased the levels of two reproductive hormones, AMH (0.14 vs. 0.09; $P < 0.05$) (Fig. 7A), and INHB (55.38 vs. 49.59; $P < 0.05$) (Fig. 7B). We found also that lactate was produced to a highly significantly level (6.00 vs. 5.71; $P < 0.001$) (Fig. 7C). Since LDH is the key enzyme to catalyze the synthesis of lactate from pyruvate under anaerobic condition [10,30], we also checked the activity of LDH in the present study. And the results showed that AA2P (250 μM, 36 h) treatment could increase the activity of LDH significantly (455.05 vs. 424.67; $P < 0.01$) (Fig. 7D). However, after checking the transcriptome sequencing data, we found that *Ldha* significantly decreased to 0.33 fold after AA2P treatment (Padj.<0.001), whereas *Ldhc* and *Ldhd* were unchanged ($P > 0.05$) (Table S6). Our results suggest that AA treatment on iSCs could also promote the secretion of vital hormones and metabolite to the growth and development of spermatogenic cells.

4. Discussion

Ascorbic acid is an essential micronutrient, capable of reducing free radicals and ROS (non-enzymatic function), and modulating the activity of ferrous ion- and 2-oxoglutarate (Fe^{2+} and 2-OG)-dependent dioxygenase family (enzymatic function) [31]. Our previous study has shown that AA could improve pig oocytic meiosis and developmental competence, through reprogramming the methylation status of DNA/RNA/histone [21]. In male animal reproduction, SCs play a crucial role in spermatogenesis by providing structural, signaling and nutritional supports [4,32], and mouse SCs under heat stress can be protected by AA supplementation [16]. However, the exact molecular mechanisms of AA on porcine iSCs are still unknown. In the present study, we confirmed that AA could exert beneficial effects on porcine iSCs in multiple aspects, possibly through modifying gene transcription to influence multiple signaling pathways, and stimulating the secretion of hormones and metabolite.

AA is transferred into the cell by two key proteins, the sodium-ascorbate co-transporters (SVCT1 and SVCT2) [33], which were found to be expressed in mouse SCs [34]. Distinct mode of *Svct1* and *Svct2* expression is linked to the specific distribution of AA in different types of cells. Here, our sequencing data showed that both *Svct1* and *Svct2* mRNA are expressed in porcine iSCs, and AA treatment significantly increased *Svct1* mRNA level, but down-regulated *Svct2*. This indicates that AA could be absorbed into porcine iSCs, and then regulates the transcriptional level of *Svct1* and *Svct2*, for which the underlying molecular circuit is unclear and needed to be studied in detail. In addition, *Ace2* was also found to be expressed in porcine iSCs, in line with the findings reported in humans [35,36]. Moreover, AA treatment induced the significant increase of *Ace2* level, and might adversely affect the male reproductive system when infected by new corona virus. However, to prove this surmise needs additional experimental evidence.

As a well-known antioxidant, AA has been shown to function via maintaining redox status in animal reproduction [37]. Our previous finding showed that AA could reduce the ROS level of porcine *in vitro* matured oocytes [21]. In rat primary SCs cultured *in vitro*, vitamin C and E together could mitigate the detrimental effect of high ROS level and cellular apoptosis caused by PM2.5 [38]. In the present study, when treating porcine iSCs with AA2P, we also found ROS and apoptosis levels could be reduced. Sequencing data showed that some DE mRNAs were enriched in the oxidoreductase activity (Sqle [39], P4ha1 [40], Ldha [41], P4ha2 [42]), and also the regulation of apoptotic process (Itga1 [43], F3 [44], ErbB4 [45], Dock 8 [46], Cth [47]). Since AA supplementation could decrease ROS and apoptotic levels, it might help promote the proliferation of porcine iSCs.

AA has been reported to be involved in epigenetic regulation [48]. AA could act as a co-factor for ten-eleven translocation (Tet) methylcytosine dioxygenase or AlkB dioxygenases, to remove the methyl group from 5-methylcytosine (5 mC) or N6-methyladenosine (m^6A) in DNA or RNA [21,49], thereby reducing the epigenetic modification and affecting gene expression. Here, we showed that AA induced the decrease of global levels for both 5 mC and m^6A, causing 1232 DE mRNAs and 937 DE lncRNAs to change more than two folds. Furthermore, in addition to act as a co-factor

Fig. 5. AA2P alters lncRNA expression and related molecular pathways. (A) Number of differentially expressed (DE) lncRNAs in AA2P-treated porcine iSCs ($|\log_2$fold change$|\geq 1$ and Padj.<0.05). (B) Heatmap clustering of AA2P-treated and control samples using lncRNA expression data. (C) GO terms significantly enriched ($P < 0.05$) from mRNA targets of DE lncRNAs. (D) Top five mRNA targets (Normalized expression≥100, starting from the smallest P value) from each of the selected GO items as listed in (C) with red frames. (E) KEGG pathways significantly enriched ($P < 0.05$). (For interpretation of the references to colour in this figure legend, the reader is referred to the Web version of this article.)

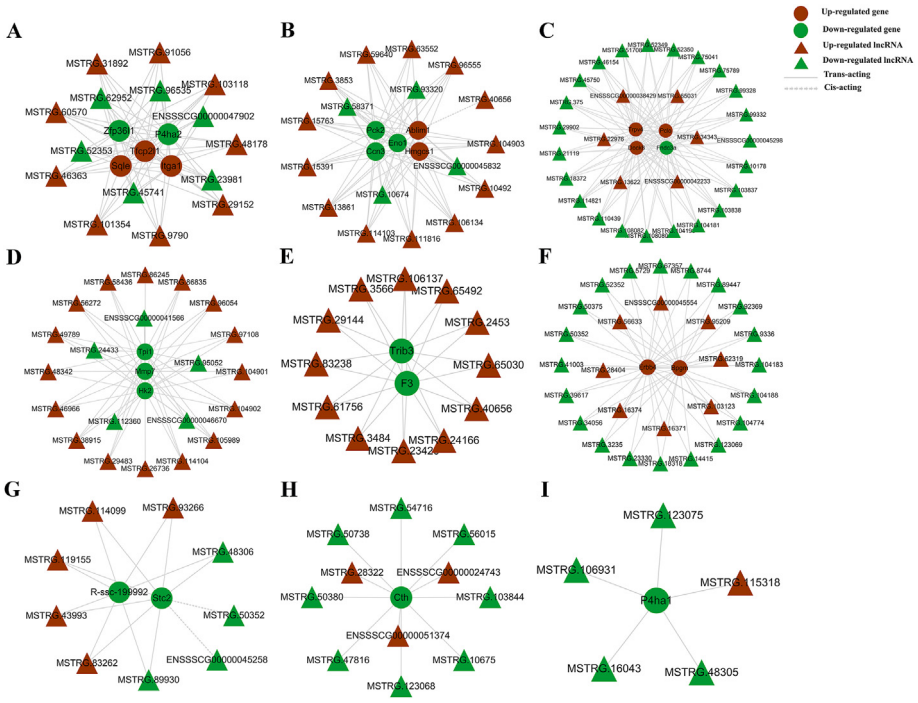

Fig. 6. Network analysis of lncRNAs and mRNAs. (A–I) Networks to show the regulatory relationship between lncRNAs (Normalized expression≥50) and the 21 DE mRNAs as listed in Fig. 4D. MSTRG represents the novel lncRNA, and ENSSSCG represents the known lncRNA.

to affect the activities of DNA/RNA (de)methyltransferases, transcriptional alteration of these enzymes induced by AA might be another way to modify the nucleic acid methylation, and subsequently influence the expression of more genes at the global level.

SCs could provide nutritional and signaling supports to spermatogenic cells via secreting growth factors, androgen binding proteins, hormones and nutrients [5,6]. Spermatogenic cells preferentially use lactate as the main energy substance to produce ATP, which could be produced from pyruvate by catalyzation of LDH in SCs [10,30]. In the present study, we showed that AA increased the lactate level, and also the LDH activity in porcine iSCs. Similarly, vitamin D3 was also shown to elevate LDH activity, and increase lactate secretion in rat iSCs [10]. These findings suggest that vitamins could be linked to the stimulation of lactate production. However, although the activity of LDH increased, we found the transcriptional level of Ldha gene decreased and those of Ldhc and Ldhd unchanged, indicating that AA did not boost LDH activity via enhancing the transcription of Ldh genes. Known as markers of SC function, AMH and INHB are glycoproteins secreted by SCs, and of fundamental roles to spermatogenesis [50]. Transcriptome sequencing in the present study also reveals that 85 and 37 DE mRNAs were enriched in the reproductive process (*Tfcp2l1, Hmgcs1, Mmp7, Fndc3a,* and *Zfp36l*1) and the regulation of hormone levels (*Pclo*, *Stc2*, *Ccn3*, *Pck2*, *Trpv4*), respectively. AA increased the secretion of AMH and INHB through modifying multiple genes related to regulation of hormone levels, but not through the direct up-regulation of Amh and Inhb transcription. Thus, the AA-induced increase of AMH and INHB in porcine iSCs indicates that AA could potentially promote male fertility through improving the function of SCs.

Various signaling pathways have been shown in SCs, to support, nourish and protect spermatogenic cells, including MAPK [51], AMPK [25], cell growth and division [52], Notch signal pathway [53], PI3k/AKT signaling pathway [54], TGF-β/Smad signaling pathway [55]. In humans with testicular cancer, SCs showed aberrant MAPK, AMPK and TGF-β/Smad signaling pathways [51]. LncRNAs was longer than 200 nt, which could not be translated into any protein, but could regulate the expression of target genes and function in multiple biological processes [56]. Recently, lncWNT3-IT has been shown to regulate WNT3 expression and affect proliferation of goat SCs, confirming the vital function of lncRNAs in SCs [57]. In the present study, we identified ten thousands of lncRNAs (most are novel), providing useful information to further elucidate their functions in porcine iSCs. Together, DE mRNAs and lncRNAs induced by AA treatment were involved in multiple signaling pathways, including MAPK, AMPK, PI3K-Akt and mTOR, as well as pathways regulating cell proliferation and cell cycle, which might help explain how AA treatment could induce multiple phenotypic changes of porcine iSCs.

5. Conclusions

Taken together, AA treatment of porcine iSCs promoted the proliferation, decreased the ROS level, inhibited apoptosis, reduced the global levels of 5 mC and m^6A of nucleic acids, and stimulated hormone and lactate secretion. AA could benefit the function of porcine iSCs via modifying gene transcription and influencing multiple signaling pathways.

Author contributions

YWY performed the experiment. LC and QM provided experimental assistance. HL provided assistance for data analysis. CXY designed the experiment and wrote the manuscript. ZQD designed the experiment and revised the manuscript.

CRediT authorship contribution statement

Yu-Wei Yang: Investigation, Data curation. **Lu Chen:** Methodology, Validation. **Qiao Mou:** Methodology. **Hao Liang:** Formal

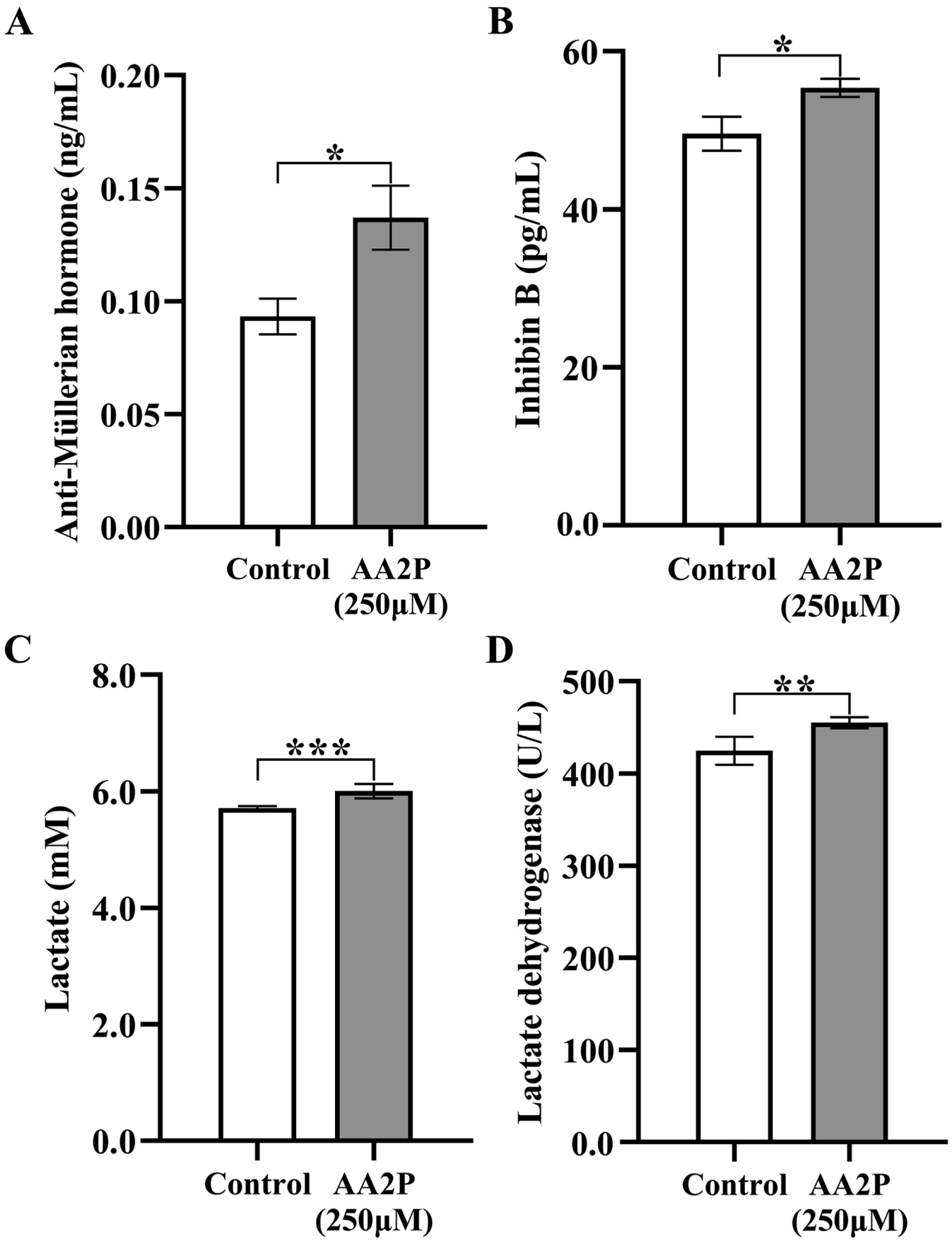

Fig. 7. AA2P and reproduction-related molecules. (A, B, C) Levels of anti-Müllerian hormone (AMH), Inhibin B (INHB) and lactate in culture media of cells treated with or without AA2P (250 μM) for 36 h. (D) Activity of the lactate dehydrogenase (LDH).

analysis, Software, Visualization. **Zhi-Qiang Du:** Conceptualization, Writing - review & editing. **Cai-Xia Yang:** Supervision, Conceptualization, Writing - original draft, preparation.

Declaration of competing interest

The authors declare that there are no conflicts of interests.

Acknowledgements

The authors appreciate the help and support from Prof. Yu-Chang Yao at Northeast Agricultural University. Funding support was provided by a Start-up grant from Yangtze University.

Appendix A. Supplementary data

Supplementary data to this article can be found online at https://doi.org/10.1016/j.theriogenology.2020.09.022.

References

[1] Sharpe RM, McKinnell C, Kivlin C, Fisher JS. Proliferation and functional maturation of Sertoli cells, and their relevance to disorders of testis function in adulthood. Reproduction 2003;125:769–84.
[2] Meroni SB, Galardo MN, Rindone G, Gorga A, Riera MF, Cigorraga SB. Molecular mechanisms and signaling pathways involved in sertoli cell proliferation. Front Endocrinol 2019;10:224.
[3] Ma C, Song H, Guan K, Zhou J, Xia X, Li F. Characterization of swine testicular cell line as immature porcine Sertoli cell line. In Vitro Cell Dev Biol Anim 2016;52:427–33.
[4] Zhang JJ, Yang WR, Wang Y, Chen L, Jeong DK, Wang XZ. Identification of microRNAs for regulating adenosine monophosphate-activated protein kinase expression in immature boar Sertoli cells in vitro. Mol Reprod Dev 2019;86:450–64.
[5] Reis MM, Moreira AC, Sousa M, Mathur PP, Oliveira PF, Alves MG. Sertoli cell as a model in male reproductive toxicology: advantages and disadvantages. J Appl Toxicol 2015;35:870–83.
[6] Zhang S, Guo J, Liang M, Qi J, Wang Z, Jian X, et al. miR-196a promotes proliferation and inhibits apoptosis of immature porcine sertoli cells. DNA Cell Biol 2019;38:41–8.
[7] Mancuso F, Arato I, Lilli C, Bellucci C, Bodo M, Calvitti M, et al. Acute effects of lead on porcine neonatal Sertoli cells in vitro. Toxicol Vitro 2018;48:45–52.
[8] Guan JY, Liao TT, Yu CL, Luo HY, Yang WR, Wang XZ. ERK1/2 regulates heat stress-induced lactate production via enhancing the expression of HSP70 in immature boar Sertoli cells. Cell Stress Chaperones 2018;23:1193–204.
[9] Luca G, Lilli C, Bellucci C, Mancuso F, Calvitti M, Arato I, et al. Toxicity of cadmium on Sertoli cell functional competence: an in vitro study. J Biol Regul Homeost Agents 2013;27:805–16.
[10] Goncalves R, Zamoner A, Zanatta L, Zanatta AP, Remor AP, da Luz Scheffer D, et al. 1,25(OH)2 vitamin D3 signalling on immature rat Sertoli cells: gamma-glutamyl transpeptidase and glucose metabolism. J Cell Commun Signal 2017;11:233–43.
[11] Aguirre-Arias MV, Velarde V, Moreno RD. Effects of ascorbic acid on spermatogenesis and sperm parameters in diabetic rats. Cell Tissue Res 2017;370:305–17.
[12] Sadeghzadeh F, Mehranjani MS, Mahmoodi M. Vitamin C ameliorates the adverse effects of dexamethasone on sperm motility, testosterone level, and spermatogenesis indexes in mice. Hum Exp Toxicol 2019;38:409–18.
[13] Gual-Frau J, Abad C, Amengual MJ, Hannaoui N, Checa MA, Ribas-Maynou J, et al. Oral antioxidant treatment partly improves integrity of human sperm DNA in infertile grade I varicocele patients. Hum Fertil 2015;18:225–9.
[14] Eidan SM. Effect on post-cryopreserved semen characteristics of Holstein bulls of adding combinations of vitamin C and either catalase or reduced glutathione to Tris extender. Anim Reprod Sci 2016;167:1–7.
[15] Gould RL, Pazdro R. Impact of supplementary amino acids, micronutrients, and overall diet on glutathione homeostasis. Nutrients 2019;11:1056.
[16] Sun J, Yin B, Tang S, Zhang X, Xu J, Bao E. Vitamin C mitigates heat damage by reducing oxidative stress, inducing HSP expression in TM4 Sertoli cells. Mol Reprod Dev 2019;86:673–85.
[17] Albokhadaim IF, Althnaian TA, El-Bahr SM. Gene expression of heat shock-proteins/factors (HSP60, HSP70, HSP90, HSF-1, HSF-3) and antioxidant enzyme activities in heat stressed broilers treated with vitamin C. Pol J Vet Sci 2019;22:565–72.
[18] DiTroia SP, Percharde M, Guerquin MJ, Wall E, Collignon E, Ebata KT, et al. Maternal vitamin C regulates reprogramming of DNA methylation and germline development. Nature 2019;573:271–5.
[19] Lee Chong T, Ahearn EL, Cimmino L. Reprogramming the epigenome with vitamin C. Front Cell Dev Biol 2019;7:128.
[20] Mallol A, Santalo J, Ibanez E. Improved development of somatic cell cloned mouse embryos by vitamin C and latrunculin A. PLoS One 2015;10:e0120033.
[21] Yu XX, Liu YH, Liu XM, Wang PC, Liu S, Miao JK, et al. Ascorbic acid induces global epigenetic reprogramming to promote meiotic maturation and developmental competence of porcine oocytes. Sci Rep 2018;8:6132.
[22] Lindsey RC, Cheng S, Mohan S. Vitamin C effects on 5-hydroxymethylcytosine and gene expression in osteoblasts and chondrocytes: potential involvement of PHD2. PloS One 2019;14:e0220653.
[23] Gao Y, Han Z, Li Q, Wu Y, Shi X, Ai Z, et al. Vitamin C induces a pluripotent state in mouse embryonic stem cells by modulating microRNA expression. FEBS J 2015;282:685–99.
[24] Zheng S, Zheng H, Huang A, Mai L, Huang X, Hu Y, et al. Piwi-interacting RNAs play a role in vitamin C-mediated effects on endothelial aging. Int J Med Sci 2020;17:946–52.
[25] Zhang L, Zhang Y, Han Z, Fang J, Chen H, Guo Z. Transcriptome analyses reveal effects of vitamin C-treated donor cells on cloned bovine embryo development. Int J Mol Sci 2019;20:2628.
[26] Yang CX, Wright EC, Ross JW. Expression of RNA-binding proteins DND1 and FXR1 in the porcine ovary, and during oocyte maturation and early embryo development. Mol Reprod Dev 2012;79:541–52.
[27] Kim D, Langmead B, Salzberg SL. HISAT: a fast spliced aligner with low memory requirements. Nat Methods 2015;12(4):357–60.
[28] Wagner GP, Kin K, Lynch VJ. Measurement of mRNA abundance using RNA-seq data: RPKM measure is inconsistent among samples. Theor Biosci 2012;131(4):281–5.
[29] Huang DW, Sherman BT, Tan Q, Collins JR, Alvord WG, Roayaei J, et al. The DAVID Gene Functional Classification Tool: a novel biological module-centric algorithm to functionally analyze large gene lists. Genome Biol 2007;8:R183.
[30] Rato L, Alves MG, Socorro S, Duarte AI, Cavaco JE, Oliveira PF. Metabolic regulation is important for spermatogenesis. Nat Rev Urol 2012;9:330–8.
[31] Lykkesfeldt J, Michels AJ, Frei B. Vitamin C. Adv Nutr 2014;5:16–8.
[32] Chen SR, Liu YX. Regulation of spermatogonial stem cell self-renewal and spermatocyte meiosis by Sertoli cell signaling. Reproduction 2015;149:R159–67.
[33] Savini I, Rossi A, Pierro C, Avigliano L, Catani MV. SVCT1 and SVCT2: key proteins for vitamin C uptake. Amino Acids 2008;34:347–55.
[34] Angulo C, Castro MA, Rivas CI, Segretain D, Maldonado R, Yanez AJ, et al. Molecular identification and functional characterization of the vitamin C transporters expressed by Sertoli cells. J Cell Physiol 2008;217:708–16.
[35] Liu X, Chen Y, Tang W, Zhang L, Chen W, Yan Z, et al. Single-cell transcriptome analysis of the novel coronavirus (SARS-CoV-2) associated gene ACE2 expression in normal and non-obstructive azoospermia (NOA) human male testes. Sci China Life Sci 2020;63:1006–15.
[36] Wang Z, Xu X. scRNA-seq profiling of human testes reveals the presence of the ACE2 receptor, A target for SARS-CoV-2 infection in spermatogonia, leydig and sertoli cells. Cells 2020;9:920.
[37] Angulo C, Maldonado R, Pulgar E, Mancilla H, Cordova A, Villarroel F, et al. Vitamin C and oxidative stress in the seminiferous epithelium. Biol Res 2011;44:169–80.
[38] Liu B, Shen LJ, Zhao TX, Sun M, Wang JK, Long CL, et al. Automobile exhaust-derived PM2.5 induces blood-testis barrier damage through ROS-MAPK-Nrf 2 pathway in sertoli cells of rats. Ecotoxicol Environ Saf 2020;189:110053.
[39] Ha J, Kwon S, Hwang JH, Park DH, Kim TW, Kang DG, et al. Squalene epoxidase plays a critical role in determining pig meat quality by regulating adipogenesis, myogenesis, and ROS scavengers. Sci Rep 2017;7:16740.
[40] Xiong G, Stewart RL, Chen J, Gao T, Scott TL, Samayoa LM, et al. Collagen prolyl 4-hydroxylase 1 is essential for HIF-1 alpha stabilization and TNBC chemoresistance. Nat Commun 2018;9:4456.
[41] Cui XG, Han ZT, He SH, Wu XD, Chen TR, Shao CH, et al. HIF1/2 alpha mediates hypoxia-induced LDHA expression in human pancreatic cancer cells. Oncotarget 2017;8:24840–52.
[42] Xiong G, Deng L, Zhu J, Rychahou PG, Xu R. Prolyl-4-hydroxylase alpha subunit 2 promotes breast cancer progression and metastasis by regulating collagen deposition. BMC Canc 2014;14:1.
[43] Gharibi A, La Kim S, Molnar J, Brambilla D, Adamian Y, Hoover M, et al. ITGA1 is a pre-malignant biomarker that promotes therapy resistance and metastatic potential in pancreatic cancer. Sci Rep 2017;7:10060.
[44] Nallathambi R, Mazuz M, Namdar D, Shik M, Namintzer D, Vinayaka AC, et al. Identification of synergistic interaction between cannabis-derived compounds for cytotoxic activity in colorectal cancer cell lines and colon polyps that induces apoptosis-related cell death and distinct gene expression. Cannabis Cannabinoid Res 2018;3:120–35.
[45] Yan F, Tan X, Wan W, Dixon BJ, Fan R, Enkhjargal B, et al. ErbB4 protects against neuronal apoptosis via activation of YAP/PIK3CB signaling pathway in a rat model of subarachnoid hemorrhage. Exp Neurol 2017;297:92–100.
[46] Crawford G, Enders A, Gileadi U, Stankovic S, Zhang Q, Lambe T, et al. DOCK8 is critical for the survival and function of NKT cells. Blood 2013;122:2052–61.
[47] Wang YH, Huang JT, Chen WL, Wang RH, Kao MC, Pan YR, et al. Dysregulation of cystathionine gamma-lyase promotes prostate cancer progression and metastasis. EMBO Rep 2019;20:e45986.
[48] Guz J, Olinski R. The role of vitamin C in epigenetic regulation. Postepy Hig Med Dosw 2017;71:747–60.
[49] Minor EA, Court BL, Young JI, Wang G. Ascorbate induces ten-eleven translocation (Tet) methylcytosine dioxygenase-mediated generation of 5-hydroxymethylcytosine. J Biol Chem 2013;288:13669–74.

[50] Iliadou PK, Tsametis C, Kaprara A, Papadimas I, Goulis DG. The Sertoli cell: novel clinical potentiality. Hormones (Basel) 2015;14:504–14.
[51] Ni FD, Hao SL, Yang WX. Multiple signaling pathways in Sertoli cells: recent findings in spermatogenesis. Cell Death Dis 2019;10:541.
[52] Gautam M, Bhattacharya I, Rai U, Majumdar SS. Hormone induced differential transcriptome analysis of Sertoli cells during postnatal maturation of rat testes. PloS One 2018;13:e0191201.
[53] Dirami G, Ravindranath N, Achi MV, Dym M. Expression of Notch pathway components in spermatogonia and Sertoli cells of neonatal mice. J Androl 2001;22:944–52.
[54] Khan SA, Ndjountche L, Pratchard L, Spicer LJ, Davis JS. Follicle-stimulating hormone amplifies insulin-like growth factor I-mediated activation of AKT/protein kinase B signaling in immature rat Sertoli cells. Endocrinology 2002;143:2259–67.
[55] Zhang X, Lui WY. Transforming growth factor-beta 3 regulates cell junction restructuring via MAPK-mediated mRNA destabilization and Smad-dependent protein degradation of junctional adhesion molecule B (JAM-B). Biochim Biophys Acta 2015;1849:601–11.
[56] Yang CX, Wang PC, Liu S, Miao JK, Liu XM, Miao YL, et al. Long noncoding RNA 2193 regulates meiosis through global epigenetic modification and cytoskeleton organization in pig oocytes. J Cell Physiol 2020. https://doi.org/10.1002/jcp.29675.
[57] He L, He Q, Qiao L, Huang S, Dai Z, Yang T, et al. LncWNT3-IT affects the proliferation of Sertoli cells by regulating the expression of the WNT3 gene in goat testis. Reprod Domest Anim 2020. https://doi.org/10.1111/rda.13738.